



Colored supramolecular charge-transfer host system using 10,10'-dihydroxy-9,9'-biphenanthryl and 2,5-disubstituted-1,4-benzoquinone

Tatsuya Ukegawa^a, Takafumi Kinuta^a, Tomohiro Sato^a, Nobuo Tajima^b, Reiko Kuroda^c,
Yoshio Matsubara^{a,*}, Yoshitane Imai^{a,*}

^a Department of Applied Chemistry, Faculty of Science and Engineering, Kinki University, 3-4-1 Kowakae, Higashi-Osaka, Osaka 577-8502, Japan

^b First-Principles Simulation Group, Computational Materials Science Center, NIMS, Sengen, Tsukuba, Ibaraki 305-0047, Japan

^c Department of Life Sciences, Graduate School of Arts and Sciences, The University of Tokyo, 3-8-1 Komaba, Meguro-ku, Tokyo 153-8902, Japan

ARTICLE INFO

Article history:

Received 21 July 2010

Received in revised form 31 August 2010

Accepted 31 August 2010

Available online 9 September 2010

Keywords:

Benzoquinone

Charge-transfer (CT) complex

10,10'-Dihydroxy-9,9'-biphenanthryl

Host–guest

Molecular recognition

ABSTRACT

A colored charge-transfer (CT) host complex is formed using racemic (*rac*)-10,10'-dihydroxy-9,9'-biphenanthryl, which has a large and widely π -conjugated phenanthrene ring, as the electron donor and 2,5-disubstituted-1,4-benzoquinone as the electron acceptor. This CT host complex can include aromatic molecules as guests and its color and diffuse reflectance spectra (DRS) change according to the type of guest molecules included. Characteristically, it is possible to tune the color and DRS of the inclusion CT complex by changing the type of the component 2,5-disubstituted-1,4-benzoquinone.

© 2010 Elsevier Ltd. All rights reserved.

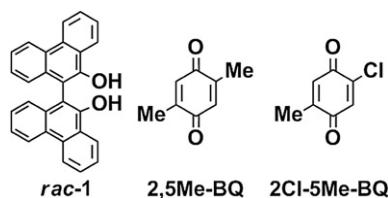
1. Introduction

The properties of organic compounds in the solid state differ from those in the solution state because molecules in the solid state are densely packed and are strongly influenced by the neighboring molecules. These properties have enabled the development of a number of solid-state supramolecular organic host compounds.¹ In recent times, there has been an increasing requirement that the chemical and physical properties of such host systems be easily tunable.² This requirement was addressed by developing two or more component supramolecular organic host systems whose properties could be easily controlled by changing the component molecules, without the need for additional synthesis.³

We have reported that supramolecular charge-transfer (CT) complexes that are composed of racemic (*rac*)-10,10'-dihydroxy-9,9'-biphenanthryl (*rac*-**1**), which has a large and widely π -conjugated phenanthrene ring, as the electron donor molecule and 2,5-dimethyl-1,4-benzoquinone (2,5Me-BQ) as the electron acceptor molecule can act as a host system.⁴ This host system, also referred to

as the *rac*-**1**/2,5Me-BQ-CT host system, can include the benzene molecule as a guest. Therefore, it is expected that the color of this host system will change according to the type of guest molecules, and its molecular recognition property can be tuned by changing the BQ moieties, without the need for additional synthesis.

In this paper, we report the preparation, the visible molecular recognition properties for different types of guest molecules, and the crystal structure of the CT host system composed of *rac*-**1** as the electron donor and 2,5-disubstituted-1,4-benzoquinone (2,5-disubstituted-BQ) as the electron acceptor. Moreover, we studied the tuning property of this CT host system by changing the 2,5-disubstituted-BQ moiety. Two types of 2,5-disubstituted-BQ, namely, 2,5Me-BQ and 2-chloro-5-methyl-1,4-benzoquinone (2Cl-5Me-BQ), were used. We studied the guest inclusion properties of this CT host system by X-ray crystallographic analysis, using two simple aromatic molecules (benzene and toluene) as guests.



* Corresponding authors. Tel.: +81 06 6730 5880x5241; fax: +81 06 6727 2024 (Y.I.); e-mail addresses: y-matsu@apch.kindai.ac.jp (Y. Matsubara), y-imai@apch.kindai.ac.jp (Y. Imai).

2. Results and discussion

First, we studied the inclusion of benzene and toluene as guest aromatic molecules in the *rac*-**1**/2,5Me-BQ-CT system. The inclusion of the toluene molecule was attempted by crystallization from a toluene solution containing *rac*-**1** and 2,5Me-BQ, which is similar to the previously reported process by which the formation of *rac*-**1**/2,5Me-BQ-CT complex including benzene (**I**) was accomplished. The toluene solution was left to stand at room temperature for 4–5 days. As expected, a colored complex **II** including toluene as a guest was obtained.

The inclusion complex **II** is deep red in color. Highly concentrated solutions of this complex are yellow in color, as same as complex **I** (Fig. ESI-1). That is, complex **II** also exhibits the deep red color only in the solid state. Moreover, the color of the CT complex is quite different from those of its component solids (*rac*-**1** and 2,5Me-BQ: light yellow). The colors of inclusion CT complexes **I** and **II** change according to the type of guest aromatic molecule. However, this is not clear from the photographs of these complexes (Fig. 1). In reality, the inclusion complex **I**, which includes benzene, is madder red in color, while complex **II**, which includes toluene, is deep red in color.



Fig. 1. Photographs of CT complexes **I** and **II**.

The diffuse reflectance spectra (DRS) of complexes **I** and **II** in the solid state are shown in Figure 2.⁵ As expected, the DRS of **I** and **II** are different from each other. The absorption edges of **I** and **II** are located at ca. 550 nm and 500 nm, respectively. These results suggest that the *rac*-**1**/2,5-disubstituted-BQ-CT host system can act as visual indicator and indicator using DRS for aromatic guest molecules in the solid state.

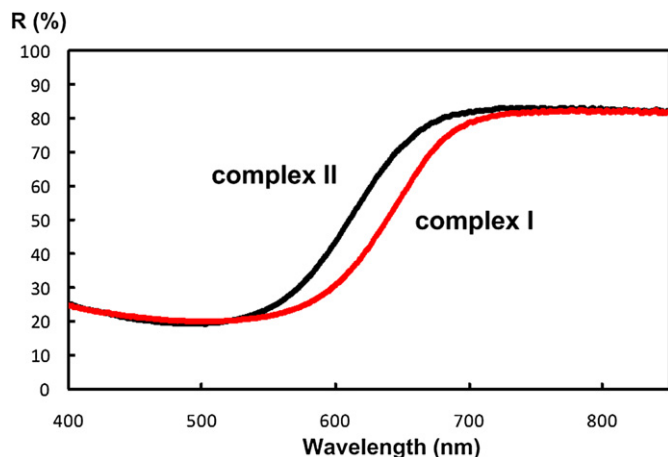


Fig. 2. DRS of complexes **I** (red line) and **II** (black line).

In order to understand the process of guest inclusion in these CT complexes and the origins of their different colors, X-ray analyses of the complexes were attempted. The crystal structure of complex **I**, which includes the benzene molecule, is shown in Figure 3.⁴

X-ray analysis revealed that the stoichiometry of **I** is (R)-**1**/(S)-**1**/2,5Me-BQ/benzene=1:1:2:1, and that the space group is *P*-1. This complex has a 1D column-like structure that is composed of (R)-**1**, (S)-

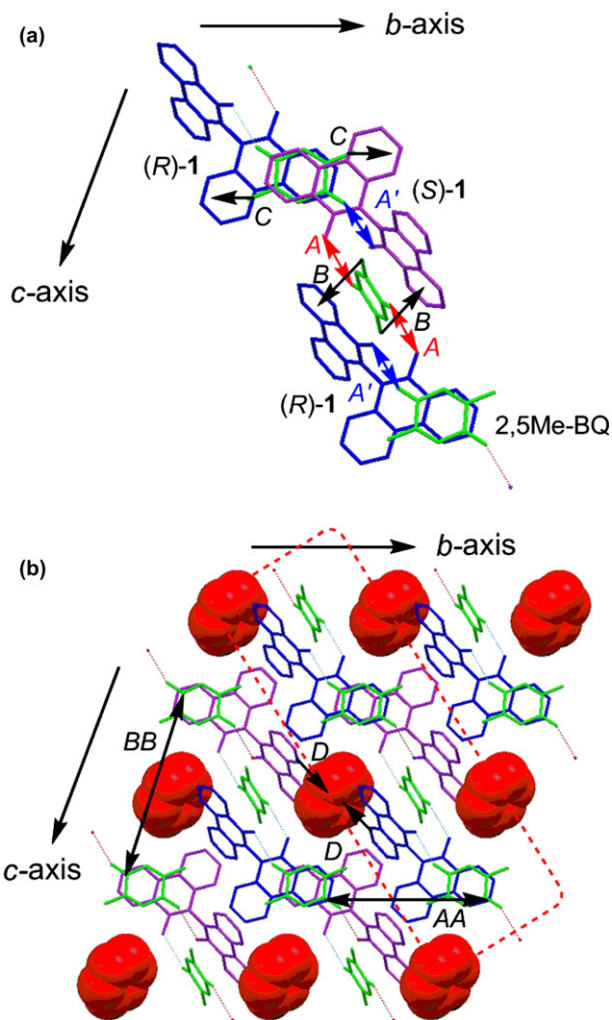


Fig. 3. Crystal structure of complex **I**. (a) 1D column-like structure observed along *a*-axis. Red arrows *A* and blue arrows *A'* indicate hydrogen bonds. Black arrows *B* and *C* indicate CH– π interactions. (b) Packing structure comprising 1D column-like structure observed along *a*-axis. Benzene is indicated by the red spacefill view. Black arrows *D* indicate phenanthrene–benzene edge-to-face interactions. The red dotted rectangle indicates the 1D column-like structure. (R)-**1**, (S)-**1**, and 2,5Me-BQ molecules are indicated in blue, purple, and green, respectively.

1, and disordered 2,5Me-BQ molecules (Fig. 3a). 2,5Me-BQ is sandwiched between the phenanthrene rings of (R)-**1** and (S)-**1** molecules. The distance of the CT interaction between the (R)-**1** [or (S)-**1**] and 2,5Me-BQ is 3.43 and 3.66 Å.⁶ The carbonyl groups of 2,5Me-BQ form hydrogen bonds with the hydroxyl groups of a phenanthrol moiety. Although the torsion angles of (R)-**1** and (S)-**1** are identical ($\pm 77.8^\circ$), the carbonyl groups of 2,5Me-BQ form hydrogen bonds of slightly different lengths with the hydroxyl groups of the phenanthrol moiety (Fig. 3a: for the hydrogen bonds indicated by red arrows *A* and blue arrows *A'*, O \cdots O are 2.71 and 2.77 Å, respectively). In addition, the CH– π interactions between the methyl group of 2,5Me-BQ and the phenanthrene ring of **1** maintain the 1D column-like structure (Fig. 3a: for the CH– π interactions indicated by black arrows *B* and *C*, 2.69 and 2.74 Å, respectively).⁷ In complex **I**, 1D channel-like cavities are formed along the *a*-axis as a result of the self-assembly of the 1D column-like structures (Fig. 3b: indicated by red dotted rectangle) without major intercolumnar interactions (Fig. 3b).⁷ Benzene guest molecules (Fig. 3b: indicated by the red spacefill view) are trapped in these cavities due to the phenanthrene–benzene edge-to-face interactions between the 5-CH of the phenanthryl ring and the benzene (Fig. 3b: for the phenanthrene–benzene edge-to-face interactions indicated by black arrows *D*, 2.92 Å).⁷

The crystal structure of complex **II**, which includes the toluene molecule, is shown in Figure 4.

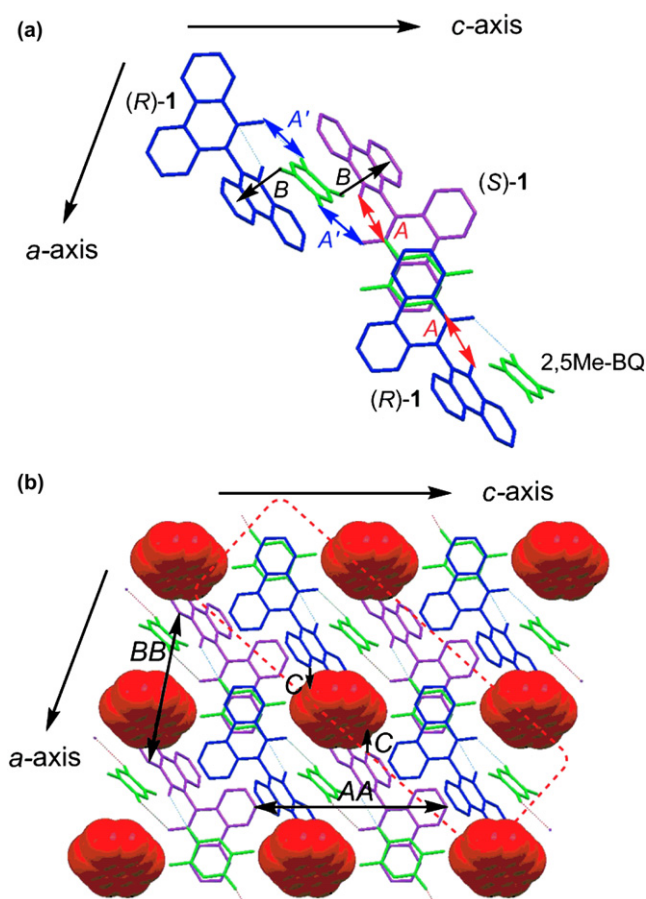


Fig. 4. Crystal structure of complex **II**. (a) 1D column-like structure observed along *b*-axis. Red arrows *A* and blue arrows *A'* indicate hydrogen bonds. Black arrows *B* indicate CH– π interactions. (b) Packing structure comprising 1D column-like structure observed along *b*-axis. Toluene is indicated by the red spacefill view. Black arrows *C* indicate phenanthrene–benzene edge-to-face interactions. The red dotted rectangle indicates the 1D column-like structure. (*R*)-**1**, (*S*)-**1**, and 2,5Me-BQ molecules are indicated in blue, purple, and green, respectively.

X-ray analysis revealed that the stoichiometry of **II** is identical to that of **I**, that is, (*R*)-**1**/*(S)*-**1**/2,5Me-BQ/toluene=1:1:2:1, and that the space group is *P*-1. This complex also has a similar 1D column-like structure with 2,5Me-BQ sandwiched by the phenanthrene rings of (*R*)-**1** and (*S*)-**1** molecules. The distance of the CT interaction between (*R*)-**1** [or (*S*)-**1**] and 2,5Me-BQ is 3.30 and 3.66 Å.⁶ The torsion angles of (*R*)-**1** and (*S*)-**1** are identical ($\pm 83.2^\circ$). The carbonyl groups of 2,5Me-BQ form hydrogen bonds of slightly different lengths with the hydroxyl groups of the phenanthrol moiety (Fig. 4a: for the hydrogen bonds indicated by red arrows *A* and blue arrows *A'*, O...O are 2.77 and 2.80 Å, respectively). Moreover, the CH– π interactions between the methyl group of 2,5Me-BQ and the phenanthrene ring of **1** maintain the 1D column-like structure (Fig. 4a: for the CH– π interactions indicated by black arrows *B*, 2.71 Å).⁷ Disordered toluene guest molecules (Fig. 4b: represented by the red spacefill view) are trapped in the 1D channel-like cavities formed as a result of the assembly of the 1D column-like structures (Fig. 4b: indicated by red dotted rectangle) due to the same phenanthrene–benzene edge-to-face interactions as in complex **I** (Fig. 4b: for the phenanthrene–benzene edge-to-face interactions indicated by black arrows *C*, 2.92 Å) (Fig. 4b).⁷

The 1D column-like structures and the packing styles of these structures are identical in complexes **I** and **II**. However, with the change in the guest molecules from benzene to toluene, the distance along the *b*-axis for **I** (or *c*-axis for **II**) (*AA*, Figs. 3b and 4b) increases from 11.06 to 12.93 Å. On the other hand, the distance along the *c*-axis for **I** (or *a*-axis for **II**) (*BB*, Figs. 3b and 4b) decreases from 12.70 to 10.49 Å. These results show that by modifying the structure and packing style of the 1D column-like structures, guest molecules can be incorporated into the 1D channel-like cavities of the *rac*-**1**/2,5Me-BQ-CT host system.

The DRS in Figure 2 suggests that the different appearance of complexes **I** and **II** results mostly from the electronic absorptions at around the absorption edge.

The spectra indicate that **I** should have lower-energy electronic absorptions than **II**. This difference of electronic absorptions is caused by changing the packing arrangement between donor and acceptor molecules, that is, donor–acceptor interactions, according to guest molecules. Then, the excited states of the CT chromophores in these complexes were calculated theoretically to understand the origins of the different electronic absorptions. The chromophores used for the calculations are molecular clusters comprising 2,5Me-BQ, (*R*)-**1**, and (*S*)-**1** that appear to be arranged in stacks as seen in the X-ray structures of the complexes (Fig. 5).

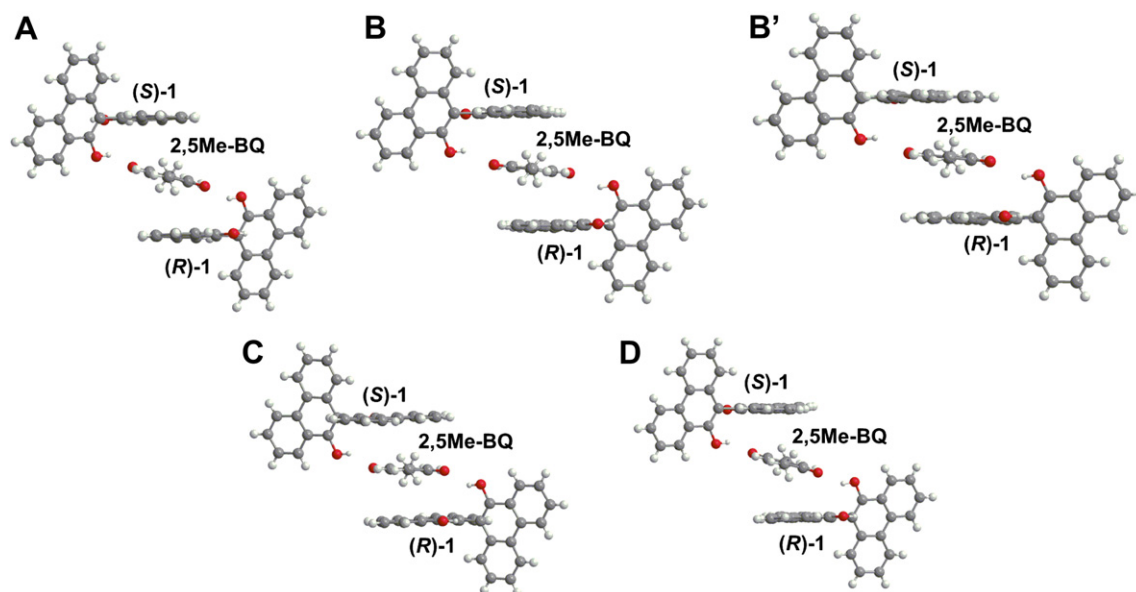


Fig. 5. Molecular clusters taken from complexes **I** and **II** for theoretical investigations (A, B, and B' from **I** and C and D from **II**).

Table 1 lists the calculated lowest energy CT excited states for the molecular clusters. The calculated results suggest that **I** should have lower-energy CT electric transitions than **II**, consistent with the experimentally observed DRS. The data suggest that the chromophore **B'** is mainly responsible for the lower-energy absorptions of **I** as compared with **II**. The small excitation energy of **B'** cannot simply be attributed to small donor–acceptor distance: The distance between the 2,5Me-BQ center and the average plane of **1** in the five clusters are 3.66 (A), 3.43 (B), 3.43 (B'), 3.30 (C), and 3.66 Å (D). It is likely that the relative orientations of molecules in **B'** are favorable for the ions 2,5Me-BQ[−] and **1**⁺ to interact strongly in the CT excited states.

Table 1
Calculated lowest energy CT excited states of molecular clusters^a

Complex I				Complex II			
	E/eV	λ/nm	f	E/eV	λ/nm	f	
Cluster A	2.79	444.9	0.1110	Cluster C	2.91	426.9	0.1610
	2.85	435.3	0.0001		2.96	419.5	0.0001
Cluster B	2.89	429.2	0.1199	Cluster D	2.84	436.5	0.1126
	2.95	420.1	0.0000		2.89	429.4	0.0000
Cluster B'	2.70	458.9	0.0000				
	2.75	451.1	0.1160				

^a Excitation energy *E*, corresponding wavelength *λ*, and oscillator strength *f*. Calculations were carried out by the ZINDO method using the geometries of X-ray structures. Each molecular cluster consists of one 2,5Me-BQ and two **1** that are arranged in a stack with this 2,5Me-BQ. Clusters **A** and **B** correspond to the (*R*)-**1**···2,5Me-BQ···(*S*)-**1** stacks in **I** along the *c*-axis and *a*-axis, respectively; clusters **C** and **D** correspond to the (*R*)-**1**···2,5Me-BQ···(*S*)-**1** stacks in **II** along the *b*-axis and *c*-axis, respectively. Clusters **B** and **B'** correspond to the different orientations of the disordered 2,5Me-BQ (see the Experimental section). See Figure 5 for the illustrations of the molecular clusters.

Next, we studied the tuning properties of the *rac*-**1**/2,5-disubstituted-BQ-CT host system by changing the 2,5-disubstituted-BQ moiety. As in the case with 2,5Me-BQ, the inclusion of the benzene and toluene molecules was attempted by crystallization from the solutions of benzene and toluene, both of which contained *rac*-**1** and 2Cl-5Me-BQ, respectively. Each solution was left to stand at room temperature. After 5–7 days, colored inclusion complexes were obtained from both systems; namely, complex **III**, including the benzene molecule, and complex **IV**, including the toluene molecule.

As expected, the color of the obtained CT complex changed according to the type of the component 2,5-disubstituted-1,4-benzoquinone. Moreover, the colors of the inclusion CT complexes **III** and **IV** also changed according to the type of guest aromatic molecule (Fig. 6). That is, the colors of the inclusion complexes **III** and **IV** were purple and deep purple, respectively. As same as complexes **I** and **II**, highly concentrated solutions of these complexes are yellow in color, (Fig. ESI-3). That is, purple and deep purple colors of complexes **III** and **IV** exhibit only in the solid state.

The DRS of complexes **III** and **IV** in the solid state differ, and they are shown in Figure 7.⁸ The absorption edges of **III** and **IV** are located at ca. 640 nm and 600 nm, respectively. These results

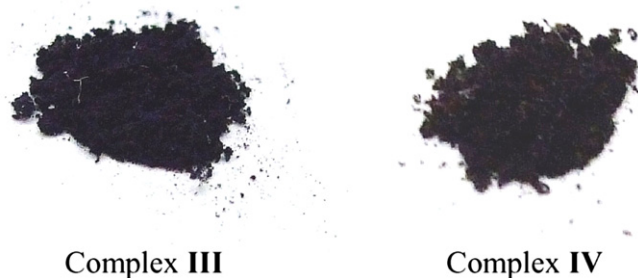


Fig. 6. Photographs of CT complexes **III** and **IV**.

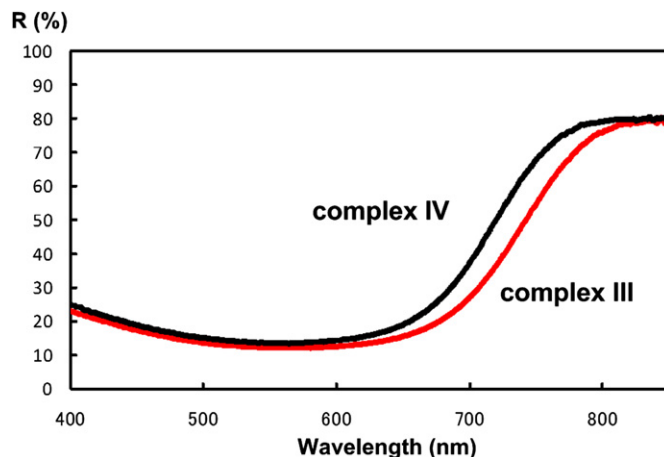


Fig. 7. DRS of complexes **III** (red line) and **IV** (black line).

suggest that the *rac*-**1**/2,5-disubstituted-BQ-CT host system can easily tune the molecular recognition properties (range of colors) of CT host complexes by changing the 2,5-disubstituted-BQ moieties and that it can function as visual indicator and indicator using DRS in the solid state.

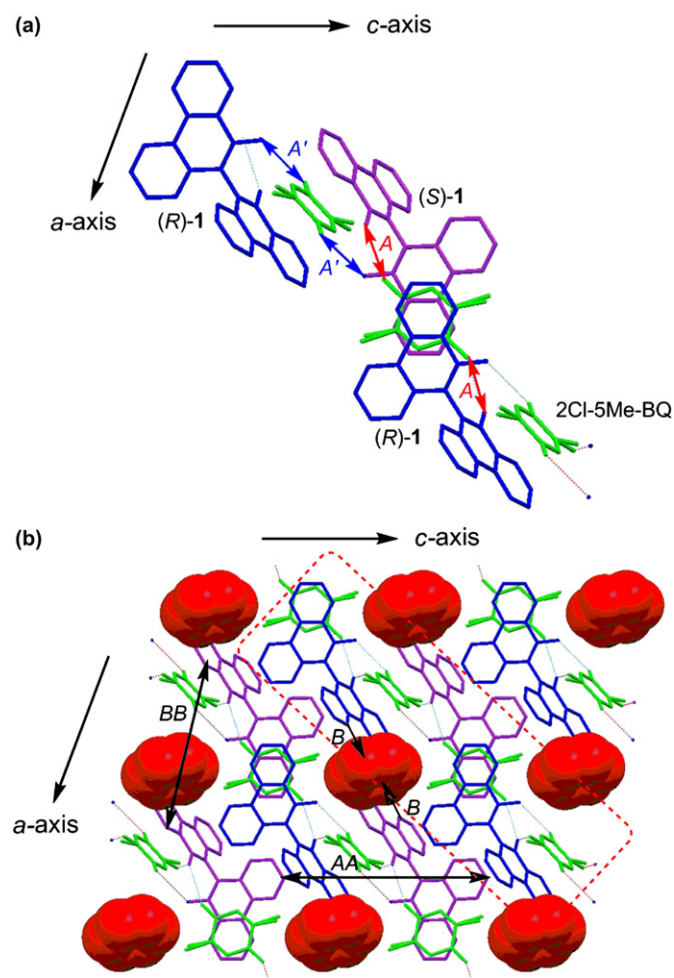


Fig. 8. Crystal structure of complex **III**. (a) 1D column-like structure observed along *a*-axis. Red arrows *A* and blue arrows *A'* indicate hydrogen bonds. (b) Packing structure comprising 1D column-like structure observed along *a*-axis. Benzene is indicated by the red spacefill view. Black arrows *B* indicate phenanthrene-benzene edge-to-face interactions. The red dotted rectangle indicates the 1D column-like structure. (*R*)-**1**, (*S*)-**1**, and 2Cl-5Me-BQ molecules are indicated in blue, purple, and green, respectively.

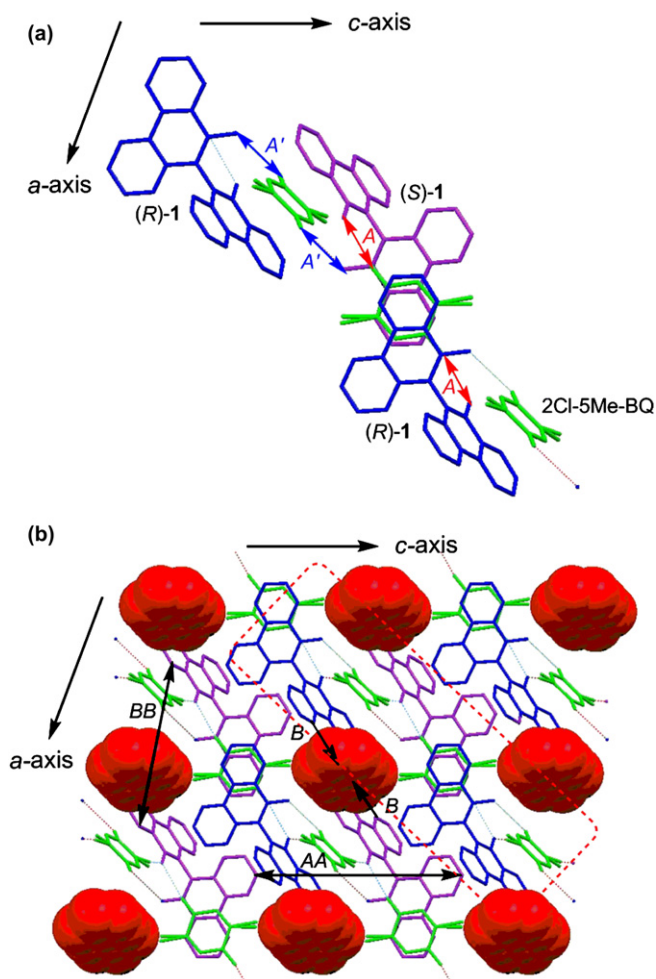


Fig. 9. Crystal structure of complex **IV**. (a) 1D column-like structure observed along *a*-axis. Red arrows *A* and blue arrows *A'* indicate hydrogen bonds. (b) Packing structure comprising 1D column-like structure observed along *a*-axis. Toluene is indicated by the red spacefill view. Black arrows *B* indicate phenanthrene-benzene edge-to-face interactions. The red dotted rectangle indicates the 1D column-like structure. (*R*)-**1**, (*S*)-**1**, and 2Cl-5Me-BQ molecules are indicated in blue, purple, and green, respectively.

In order to study the process of guest inclusion and the origin of color in **III** and **IV**, we carried out the X-ray crystallographic analyses of complexes **III** and **IV**. The crystal structures of complexes **III** and **IV** are shown in Figures 8 and 9. Similar to the 1/2,5Me-BQ-CT host system, the crystal structures of complexes **III** and **IV** are identical. X-ray analyses revealed that the stoichiometry of **III** and **IV** is (*R*)-**1**/*(S)*-**1**/2Cl-5Me-BQ/benzene (or toluene)=1:1:2:1, and that the space group is *P*-1. These complexes also have a shared 1D column-like structure composed of (*R*)-**1**, (*S*)-**1**, and disordered 2Cl-5Me-BQ molecules (Figs. 8a and 9a).

2Cl-5Me-BQ is sandwiched between the phenanthrene rings of (*R*)-**1** and (*S*)-**1** molecules.

The distance of the CT interaction between the interacting (*R*)-**1** [or (*S*)-**1**] and 2Cl-5Me-BQ is 3.35 Å for **III** and 3.26 Å for **IV**, respectively.⁶ The torsion angles of (*R*)-**1** and (*S*)-**1** are identical ($\pm 83.2^\circ$ for **III** and $\pm 84.0^\circ$ for **IV**). The carbonyl groups of 2Cl-5Me-BQ form hydrogen bonds of slightly different lengths with the hydroxyl groups of the phenanthrol moiety. In complex **III**, their distances are 2.75 and 2.76 Å, as indicated by the red arrows *A* and the blue arrows *A'* in Figure 8a. In complex **IV**, their distances are 2.77 and 2.80 Å, as indicated by the red arrows *A* and the blue arrows *A'* in Figure 9a. In contrast to complexes **I** and **II**, no CH- π interactions were observed between the methyl group of 2Cl-5Me-

BQ and the phenanthrene ring of **1**.⁷ Although toluene guest molecules are disordered, in both complexes, guest aromatic molecules (Figs. 8b and 9b: indicated by the red spacefill view) are trapped in 1D channel-like cavities formed as a result of the assembly of 1D column-like structures (Figs. 8b and 9b: indicated by red dotted rectangle) because of the phenanthrene-benzene edge-to-face interactions similar to those in complexes **I** and **II** (Figs. 8b and 9b: indicated by black arrows *B*, 2.83 Å for **III** and 2.93 Å for **IV**) (Figs. 8b and 9b).⁷

Although the 1D column-like structures and the packing styles of these structures are identical in complexes **III** and **IV**, when the guest molecule is changed from benzene to toluene, the intercolumnar distance between the 1D column-like structures along the *c*-axis (*AA*, Figs. 8b and 9b) increases from 12.57 to 12.81 Å. On the other hand, the intercolumnar distance between the 1D column-like structures along the *a*-axis (*BB*, Figs. 8b and 9b) decreases from 10.52 to 10.43 Å. These results show that by modifying the packing style of the 1D column-like structures, guest molecules can be incorporated into the 1D channel-like cavities of the 1/2Cl-5Me-BQ-host system in the same manner as done in the case of the 1/2,5Me-BQ-CT host system.

Comparing the DRS of the 1/2,5Me-BQ and 1/2Cl-5Me-BQ complexes, it is seen that the absorption edge shifts to longer wavelengths (from 500–550 nm for 1/2,5Me-BQ to 600–640 nm for 1/2Cl-5Me-BQ). The electron affinities of 2,5Me-BQ and 2Cl-5Me-BQ are 1.32 and 1.65 eV, respectively. As the electron affinity of the BQ derivative becomes stronger (from 2,5Me-BQ (lowest affinity) to 2Cl-5Me-BQ (highest affinity)), the absorption edges shift to longer wavelengths. Since the 1D column-like structures and the packing styles of the four complexes **I–IV** are identical, the tuning properties affecting the colors of this CT host system would reflect the electron acceptor properties of 2,5-disubstituted-BQ.

3. Conclusion

A supramolecular CT host system composed of *rac*-**1** as the electron donor and 2,5-disubstituted-BQ as the electron acceptor was developed. From X-ray crystallographic analyses, it was found that the CT host system can include benzene or toluene as guests after tuning its 1D column-like structure composed of *rac*-**1** and 2,5-disubstituted-BQ and its packing. The color and the DRS of the inclusion CT complex are sensitive to the type of guest molecules included. As is characteristic of this supramolecular CT host system, the molecular recognition ability of the CT complexes can be tuned by changing the type of 2,5-disubstituted-BQ used. The unique abilities of this CT host system, which has a large and widely π -conjugated phenanthrene ring, further enhance its potential applications; for example, it can be used as a novel visual indicator in the solid state for molecular recognition.

4. Experimental

4.1. General methods

Compound *rac*-**1** was synthesized by previously reported method.⁹ 2,5Me-BQ and 2Cl-5Me-BQ were purchased from Tokyo Kasei Kogyo Co. Guest benzene and toluene solutions were purchased from Wako Pure Chemical Industry.

4.2. Formation of supramolecular CT host complex

The inclusion of benzene (toluene) molecules was attempted by crystallization from a benzene (toluene) solution containing *rac*-**1** and 2,5Me-BQ (or 2Cl-5Me-BQ). Compound *rac*-**1** (16 mg, 0.04 mmol) and 2,5Me-BQ (or 2Cl-5Me-BQ) (0.12 mmol) molecules were dissolved in the benzene (or toluene) solution (4–5 mL) by

heating. Each solution was allowed to stand at room temperature. After 4–7 days, the respective colored crystals **I** containing benzene from the *rac*-1/2,5Me-BQ system (10 mg), **II** containing toluene from the *rac*-1/2,5Me-BQ system (15 mg), **III** containing benzene from the *rac*-1/2Cl-5Me-BQ system (14 mg), and **IV** containing toluene from the *rac*-1/2Cl-5Me-BQ system (14 mg) were deposited and collected. The weights mentioned for each type of crystal are the weights of the total crop of crystals obtained in a single batch.

4.3. Measurement of DRS of CT complexes

DRS of crystals were measured with a HITACHI U-4000 Spectrometer.

4.4. X-ray crystallographic study of crystal

X-ray diffraction data for single crystals were collected using BRUKER APEX. The crystal structures were solved by the direct method¹⁰ and refined by full-matrix least-squares using SHELXL97.¹⁰ The diagrams were prepared using PLATON.¹¹ Absorption corrections were performed using SADABS.¹² Nonhydrogen atoms were refined with anisotropic displacement parameters, and hydrogen atoms were included in the models in their calculated positions in the riding model approximation. *Crystallographic data for I*: $C_{28}H_{18}O_2 \cdot C_8H_8O_2 \cdot 0.5C_6H_6$, $M=561.62$, triclinic, space group *P*-1, $a=10.7984(18)$, $b=11.0571(19)$, $c=12.696(2)$ Å, $\alpha=106.224(3)$, $\beta=90.705(3)$, $\gamma=103.874(3)^\circ$, $V=1408.0(4)$ Å³, $Z=2$, $D_c=1.325$ g cm⁻³, $\mu(Mo K\alpha)=0.085$ mm⁻¹, 12,177 reflections measured, 6205 unique, final $R(F^2)=0.0582$ using 5084 reflections with $I>2.0\sigma(I)$, $R(\text{all data})=0.0722$, $T=115(2)$ K. CCDC 754621. *Crystallographic data for II*: $C_{28}H_{18}O_2 \cdot C_8H_8O_2 \cdot 0.5C_7H_8$, $M=568.64$, triclinic, space group *P*-1, $a=10.4887(7)$, $b=11.0375(7)$, $c=12.9292(8)$ Å, $\alpha=92.3540(10)$, $\beta=101.2660(10)$, $\gamma=100.6370(10)^\circ$, $V=1438.11(16)$ Å³, $Z=2$, $D_c=1.313$ g cm⁻³, $\mu(Mo K\alpha)=0.084$ mm⁻¹, 12,689 reflections measured, 6409 unique, final $R(F^2)=0.0511$ using 5303 reflections with $I>2.0\sigma(I)$, $R(\text{all data})=0.0607$, $T=115(2)$ K. CCDC 770501. *Crystallographic data for III*: $C_{28}H_{18}O_2 \cdot C_7H_6O_2Cl \cdot 0.5C_6H_6$, $M=582.04$, triclinic, space group *P*-1, $a=10.5191(13)$, $b=10.9184(14)$, $c=12.5725(16)$ Å, $\alpha=92.405(2)$, $\beta=102.763(2)$, $\gamma=101.650(2)^\circ$, $V=1373.6(3)$ Å³, $Z=2$, $D_c=1.407$ g cm⁻³, $\mu(Mo K\alpha)=0.184$ mm⁻¹, 11,155 reflections measured, 5521 unique, final $R(F^2)=0.0783$ using 4008 reflections with $I>2.0\sigma(I)$, $R(\text{all data})=0.1075$, $T=115(2)$ K. CCDC 770502. *Crystallographic data for IV*: $C_{28}H_{18}O_2 \cdot C_7H_6O_2Cl \cdot 0.5C_7H_8$, $M=589.05$, triclinic, space group *P*-1, $a=10.4340(7)$, $b=11.0515(7)$, $c=12.8073(8)$ Å, $\alpha=92.5800(10)$, $\beta=100.9660(10)$, $\gamma=100.7600(10)^\circ$, $V=1419.39(16)$ Å³, $Z=2$, $D_c=1.378$ g cm⁻³, $\mu(Mo K\alpha)=0.179$ mm⁻¹, 12,401 reflections measured, 6325 unique, final $R(F^2)=0.0554$ using 5213 reflections with $I>2.0\sigma(I)$, $R(\text{all data})=0.0668$, $T=115(2)$ K. CCDC 770503. These data can be obtained free of charge via www.ccdc.cam.ac.uk/conts/retrieving.html (or from the Cambridge Crystallographic Data Centre, 12, Union Road, Cambridge CB21EZ, UK; fax: +44 1223 336 033; deposit@ccdc.cam.ac.uk).

4.5. Theoretical calculations of the excited states of CT chromophores

The excited states of CT chromophores in complexes **I** and **II** were calculated by the ZINDO method.¹³ The chromophores used for calculations are molecular clusters consisting of one 2,5Me-BQ and two **1** that appear to be arranged in stacks, according to the X-ray structures of the complexes (Fig. 5). Two different clusters, which correspond to the two symmetrically independent 2,5Me-BQs, were examined for each complex. Clusters **A** and **B** correspond to the (R)-**1**⋯2,5Me-BQ⋯(S)-**1** stacks in **I** along *c*-axis and *a*-axis, respectively; clusters **C** and **D** correspond to the (R)-**1**⋯2,5Me-BQ⋯(S)-**1** stacks in **II** along the *b*-axis and *c*-axis, respectively. One of the 2,5Me-BQs in crystal **I** (2,5Me-BQ in cluster **B**) has a disorder of two

molecular orientations. Two clusters were created from the respective molecular orientations (clusters **B** and **B'**). The Gaussian 03 program¹⁴ was used to perform these quantum chemical calculations (along with the calculations in Section 4.6).

4.6. Theoretical calculations of electron affinities of BQ derivatives

The electron affinities of the two 2,5-disubstituted-BQ derivatives were calculated using the hybrid density functional theory (B3LYP)¹⁵ with the cc-pVDZ basis set.¹⁶

Acknowledgements

This work was supported by a Grant-in-Aid for Scientific Research (No. 22750133) from the Ministry of Education, Culture, Sports, Science and Technology, Japan, and Foundation for Promotion of Material Science and Technology (MST). T.K. is grateful to JSPS Research Fellowships for Young Scientists.

Supplementary data

Supplementary data associated with this article can be found in the online version, at doi:10.1016/j.tet.2010.08.074. These data include MOL files and InChIKeys of the most important compounds described in this article.

References and notes

- (a) *Inclusion Compounds*; Atwood, J. L., Davies, J. E. D., MacNicol, D. D., Eds.; Academic: New York, NY, 1984; Vols. 1–3; (b) Walba, D. M.; Clark, N. A.; Razavi, H. A.; Parmar, D. S. In *Inclusion Phenomenon and Molecular Recognition*; Atwood, J. L., Ed.; Plenum: New York, NY, 1990; (c) *Comprehensive Supramolecular Chemistry*; Lehn, J.-M., Atwood, J. L., Davies, J. E. D., MacNicol, D. D., Vogtle, F., Eds.; Pergamon: Oxford, 1996; Vols. 1–11; (d) *Encyclopedia of Supramolecular Chemistry*; Atwood, J. L., Steed, J. W., Eds.; Marcel Dekker: New York, NY, 2004; (e) *Perspectives in Supramolecular Chemistry*; Toda, F., Bishop, R., Eds.; John Wiley & Sons: Chichester, UK, 2004; Vol. 8; and reference cited therein.
- (a) Ochiai, K.; Mazaki, Y.; Kobayashi, K. *Tetrahedron Lett.* **1995**, 36, 5947; (b) Ochiai, K.; Mazaki, Y.; Nishikori, S.; Kobayashi, K.; Hayashi, S. *J. Chem. Soc., Perkin Trans. 2* **1996**, 1139; (c) Ochiai, K.; Mazaki, Y.; Kobayashi, K. *Mol. Cryst. Liq. Cryst.* **1996**, 276, 153; (d) Mizobe, Y.; Miyata, M.; Hisaki, I.; Hasegawa, Y.; Tohnai, N. *Org. Lett.* **2006**, 8, 4295; (e) Kodama, K.; Kobayashi, Y.; Saigo, K. *Chem.—Eur. J.* **2007**, 13, 2144; (f) Kodama, K.; Kobayashi, Y.; Saigo, K. *Cryst. Growth Des.* **2007**, 7, 935 and reference cited therein.
- (a) Imai, Y.; Sato, T.; Kuroda, R. *Chem. Commun.* **2005**, 3289; (b) Imai, Y.; Tajima, N.; Sato, T.; Kuroda, R. *Org. Lett.* **2006**, 8, 2941; (c) Imai, Y.; Kawaguchi, K.; Sato, T.; Kuroda, R.; Matsubara, Y. *Tetrahedron Lett.* **2006**, 47, 7885; (d) Imai, Y.; Murata, K.; Kawaguchi, K.; Sato, T.; Kuroda, R.; Matsubara, Y. *Org. Lett.* **2007**, 9, 3457; (e) Imai, Y.; Kamon, K.; Kinuta, T.; Tajima, N.; Sato, T.; Kuroda, R.; Matsubara, Y. *Tetrahedron Lett.* **2007**, 48, 6321; (f) Imai, Y.; Kido, S.; Kamon, K.; Kinuta, T.; Tajima, N.; Sato, T.; Kuroda, R.; Matsubara, Y. *Org. Lett.* **2007**, 9, 5047; (g) Imai, Y.; Kamon, K.; Kinuta, T.; Tajima, N.; Sato, T.; Kuroda, R.; Matsubara, Y. *Tetrahedron* **2007**, 63, 11928; (h) Shiota, N.; Kinuta, T.; Sato, T.; Tajima, N.; Kuroda, R.; Matsubara, Y.; Imai, Y. *Cryst. Growth Des.* **2010**, 10, 1341; (i) Kinuta, T.; Kamon, K.; Tajima, N.; Sato, T.; Kuroda, R.; Matsubara, Y.; Imai, Y. *Supramol. Chem.* **2010**, 22, 221; (j) Kinuta, T.; Tajima, N.; Sato, T.; Kuroda, R.; Matsubara, Y.; Imai, Y. *J. Mol. Struct.* **2010**, 964, 27 and references cited therein.
- Ukegawa, T.; Kinuta, T.; Sato, T.; Tajima, N.; Kuroda, R.; Matsubara, Y.; Imai, Y. *Chem. Lett.* **2010**, 39, 257.
- Optical absorption spectra (the Kubelka–Munk functions derived from the DRS) of CT complexes **I** and **II** are shown in Figure ESI-2.
- Distance between the center of 2,5-disubstituted-BQ and the average plane of the phenanthrol 14-membered ring.
- It is determined by PLATON geometry calculation.
- Optical absorption spectra (the Kubelka–Munk functions derived from the DRS) of CT complexes **III** and **IV** are shown in Figure ESI-4.
- Noji, M.; Nakajima, M.; Koga, K. *Tetrahedron Lett.* **1994**, 35, 7983.
- Sheldrick, G. M. *Acta Crystallogr., Sect. A* **2008**, 64, 112.
- Spek, A. L. *PLATON, Molecular geometry and graphics program*; University of Utrecht: The Netherlands, 1999.
- Sheldrick, G. M. *SADABS, Program for Empirical Absorption Correction of Area Detector Data*; University of Göttingen: Germany, 1996.

13. (a) Ridley, J. E.; Zerner, M. C. *Theor. Chim. Acta* **1973**, *32*, 111; (b) Ridley, J. E.; Zerner, M. C. *Theor. Chim. Acta* **1976**, *42*, 223; (c) Zerner, M. C.; Lowe, G. H.; Kirchner, R. F.; Mueller-Westerhoff, U. T. *J. Am. Chem. Soc.* **1980**, *102*, 589.
14. Frisch, M. J.; Trucks, G. W.; Schlegel, H. B.; Scuseria, G. E.; Robb, M. A.; Cheeseman, J. R.; Montgomery, J. A., Jr.; Vreven, T.; Kudin, K. N.; Burant, J. C.; Millam, J. M.; Iyengar, S. S.; Tomasi, J.; Barone, V.; Mennucci, B.; Cossi, M.; Scalmani, G.; Rega, N.; Petersson, G. A.; Nakatsuji, H.; Hada, M.; Ehara, M.; Toyota, K.; Fukuda, R.; Hasegawa, J.; Ishida, M.; Nakajima, T.; Honda, Y.; Kitao, O.; Nakai, H.; Klene, M.; Li, X.; Knox, J. E.; Hratchian, H. P.; Cross, J. B.; Bakken, V.; Adamo, C.; Jaramillo, J.; Gomperts, R.; Stratmann, R. E.; Yazyev, O.; Austin, A. J.; Cammi, R.; Pomelli, C.; Ochterski, J. W.; Ayala, P. Y.; Morokuma, K.; Voth, G. A.; Salvador, P.; Dannenberg, J. J.; Zakrzewski, V. G.; Dapprich, S.; Daniels, A. D.; Strain, M. C.; Farkas, O.; Malick, D. K.; Rabuck, A. D.; Raghavachari, K.; Foresman, J. B.; Ortiz, J. V.; Cui, Q.; Baboul, A. G.; Clifford, S.; Cioslowski, J.; Stefanov, B. B.; Liu, G.; Liashenko, A.; Piskorz, P.; Komaromi, I.; Martin, R. L.; Fox, D. J.; Keith, T.; Al-Laham, M. A.; Peng, C. Y.; Nanayakkara, A.; Challacombe, M.; Gill, P. M. W.; Johnson, B.; Chen, W.; Wong, M. W.; Gonzalez, C.; Pople, J. A. *Gaussian 03, Revision C.02*; Gaussian: Wallingford, CT, 2004.
15. Becke, A. D. *J. Chem. Phys.* **1993**, *98*, 5648.
16. (a) Dunning, T. H., Jr. *J. Chem. Phys.* **1989**, *90*, 1007; (b) Woon, D. E.; Dunning, T. H., Jr. *J. Chem. Phys.* **1993**, *98*, 1358; (c) Wilson, A. K.; Woon, D. E.; Peterson, K. A.; Dunning, T. H., Jr. *J. Chem. Phys.* **1999**, *110*, 7667.